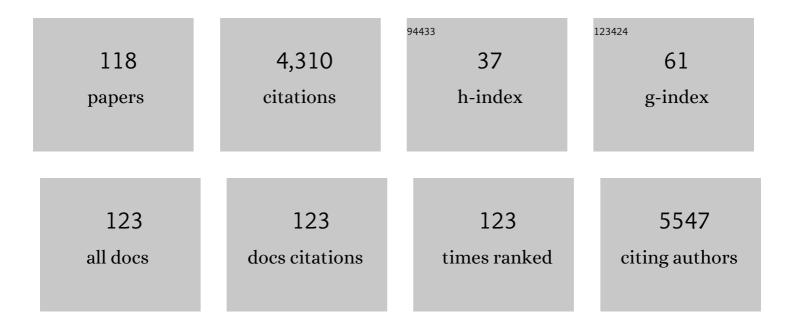
Sang Uck Lee

List of Publications by Year in descending order

Source: https://exaly.com/author-pdf/2201215/publications.pdf Version: 2024-02-01



| # | Article | IF | CITATIONS |
|----|--|----------------|-----------|
| 1 | Strain-induced carrier mobility modulation in organic semiconductors. Journal of Industrial and Engineering Chemistry, 2022, 107, 137-144. | 5.8 | 2 |
| 2 | Guanidinium-Pseudohalide Perovskite Interfaces Enable Surface Reconstruction of Colloidal Quantum Dots for Efficient and Stable Photovoltaics. ACS Nano, 2022, 16, 1649-1660. | 14.6 | 18 |
| 3 | Designing a descriptor for the computational screening of argyrodite-based solid-state superionic conductors: uniformity of ion-cage size. Journal of Materials Chemistry A, 2022, 10, 7888-7895. | 10.3 | 7 |
| 4 | Designing and Tuning the Electronic Structure of Nickel–Vanadium Layered Double Hydroxides for Highly Efficient Oxygen Evolution Electrocatalysis. ACS Catalysis, 2022, 12, 3821-3831. | 11.2 | 58 |
| 5 | Hybridized heterostructure of CoS and MoS2 nanoparticles for highly-efficient and robust bifunctional water electrolysis. Applied Surface Science, 2022, 592, 153196. | 6.1 | 17 |
| 6 | Structural and Electronic Modulations of Imidazolium Covalent Organic Framework-Derived Electrocatalysts for Oxygen Redox Reactions in Rechargeable Zn–Air Batteries. ACS Applied Materials & Interfaces, 2022, 14, 24404-24414. | 8.0 | 12 |
| 7 | Highâ€Alkaline Waterâ€Splitting Activity of Mesoporous 3D Heterostructures: An Amorphousâ€Shell@Crystallineâ€Core Nanoâ€Assembly of Coâ€Niâ€Phosphate Ultrathinâ€Nanosheets and V― Cobaltâ€Nitride Nanowires. Advanced Science, 2022, 9, . | D ¤p æd | 41 |
| 8 | Stable performance of Li-S battery: Engineering of Li2S smart cathode by reduction of multilayer graphene-embedded 2D-MoS2. Journal of Alloys and Compounds, 2021, 862, 158031. | 5.5 | 11 |
| 9 | Mechanically robust, self-healing graphene like defective SiC: A prospective anode of Li-ion batteries. Applied Surface Science, 2021, 541, 148417. | 6.1 | 25 |
| 10 | Single-atom oxygen reduction reaction electrocatalysts of Fe, Si, and N co-doped carbon with 3D interconnected mesoporosity. Journal of Materials Chemistry A, 2021, 9, 4297-4309. | 10.3 | 43 |
| 11 | State of charge dependent ordered and disordered phases in a Li[Ni1/3Co1/3Mn1/3]O2 cathode material. Materials Advances, 2021, 2, 3965-3970. | 5.4 | 2 |
| 12 | Lowâ€Dimensional Singleâ€Cation Formamidinium Lead Halide Perovskites (FA <i>_m</i> ₊₂ Pb <i>_m</i> Br ₃ <i>_m+2 From Synthesis to Rewritable Phaseâ€Change Memory Film. Advanced Functional Materials, 2021, 31, 2011093.</i> |): 14.9 | 12 |
| 13 | Phaseâ€Change Memory Films: Lowâ€Dimensional Singleâ€Cation Formamidinium Lead Halide Perovskites (FA <i>_m</i> ₊₂ Pb <i>_m</i> Sub> _a <i>_m</i> From Synthesis to Rewritable Phaseâ€Change Memory Film (Adv. Funct. Mater. 17/2021). Advanced Functional Materials. 2021. 31. 2170118. |): 14.9 | 1 |
| 14 | Bifunctional Covalent Organic Frameworkâ€Derived Electrocatalysts with Modulated <i>p</i> â€Band Centers for Rechargeable Zn–Air Batteries. Advanced Functional Materials, 2021, 31, 2101727. | 14.9 | 76 |
| 15 | Ampere-hour-scale zinc–air pouch cells. Nature Energy, 2021, 6, 592-604. | 39.5 | 149 |
| 16 | Nanoporous <scp>Titaniumâ€Oxo</scp> Molecular Cluster for <scp>CO₂</scp> Selective Adsorption. Bulletin of the Korean Chemical Society, 2021, 42, 1014-1019. | 1.9 | 2 |
| 17 | Efficient organic manganese(<scp>ii</scp>) bromide green-light-emitting diodes enabled by manipulating the hole and electron transport layer. Journal of Materials Chemistry C, 2021, 9, 11314-11323. | 5.5 | 20 |
| 18 | Unveiling the effect of the crystalline phases of iron oxyhydroxide for highly sensitive and selective detection of dopamine. Dalton Transactions, 2021, 50, 13497-13504. | 3.3 | 5 |

| # | Article | IF | CITATIONS |
|----|--|------|-----------|
| 19 | Experimental and Theoretical Insights into the Borohydride-Based Reduction-Induced Metal Interdiffusion in Fe-Oxide@NiCo ₂ O ₄ for Enhanced Oxygen Evolution. ACS Applied Materials & Interfaces, 2021, 13, 53725-53735. | 8.0 | 32 |
| 20 | Experimental and Theoretical Insights into Transition-Metal (Mo, Fe) Codoping in a Bifunctional Nickel Phosphide Microsphere Catalyst for Enhanced Overall Water Splitting. ACS Applied Energy Materials, 2021, 4, 14169-14179. | 5.1 | 39 |
| 21 | Temperature-dependent lithium diffusion in phographene: Insights from molecular dynamics simulation. Journal of Industrial and Engineering Chemistry, 2020, 81, 287-293. | 5.8 | 10 |
| 22 | Rational design of a PC3 monolayer: A high-capacity, rapidly charging anode material for sodium-ion batteries. Carbon, 2020, 157, 420-426. | 10.3 | 49 |
| 23 | Role of Transition Metals in Layered Double Hydroxides for Differentiating the Oxygen Evolution and Nonenzymatic Glucose Sensing. ACS Applied Materials & Interfaces, 2020, 12, 6193-6204. | 8.0 | 48 |
| 24 | Donor–Acceptor-Appended Triarylboron Lewis Acids: Ratiometric or Time-Resolved Turn-On Fluorescence Response toward Fluoride Binding. Inorganic Chemistry, 2020, 59, 1414-1423. | 4.0 | 11 |
| 25 | A Robust Nonprecious CuFe Composite as a Highly Efficient Bifunctional Catalyst for Overall Electrochemical Water Splitting. Small, 2020, 16, e1905884. | 10.0 | 63 |
| 26 | Enhancing the thermally activated delayed fluorescence of nido-carborane-appended triarylboranes by steric modification of the phenylene linker. Inorganic Chemistry Frontiers, 2020, 7, 3456-3464. | 6.0 | 13 |
| 27 | Strain induced structural transformation, mechanical and phonon stability in silicene derived 2D-SiB. Journal of Industrial and Engineering Chemistry, 2020, 90, 399-406. | 5.8 | 5 |
| 28 | Frustrated Lewis pairs with thermally activated delayed fluorescence properties: activation of formaldehyde. Dalton Transactions, 2020, 49, 13198-13201. | 3.3 | 1 |
| 29 | Hybridisation of perovskite nanocrystals with organic molecules for highly efficient liquid scintillators. Light: Science and Applications, 2020, 9, 156. | 16.6 | 85 |
| 30 | Strain-induced work function in h-BN and BCN monolayers. Physica E: Low-Dimensional Systems and Nanostructures, 2020, 123, 114180. | 2.7 | 42 |
| 31 | Tuning d-band centers by coupling PdO nanoclusters to WO ₃ nanosheets to promote the oxygen reduction reaction. Journal of Materials Chemistry A, 2020, 8, 13490-13500. | 10.3 | 33 |
| 32 | Complementary Hybrid Semiconducting Superlattices with Multiple Channels and Mutual Stabilization. Nano Letters, 2020, 20, 4864-4871. | 9.1 | 13 |
| 33 | Molecular engineering of nanostructures and activities on bifunctional oxygen electrocatalysts for Zinc-air batteries. Applied Catalysis B: Environmental, 2020, 270, 118869. | 20.2 | 34 |
| 34 | Densely colonized isolated Cu-N single sites for efficient bifunctional electrocatalysts and rechargeable advanced Zn-air batteries. Applied Catalysis B: Environmental, 2020, 268, 118746. | 20.2 | 110 |
| 35 | Designing a high-performance nitrogen-doped titanium dioxide anode material for lithium-ion batteries by unravelling the nitrogen doping effect. Nano Energy, 2020, 74, 104829. | 16.0 | 38 |
| 36 | Bias-Dependent Multichannel Transport in Graphene–Boron Nitride Heterojunction Nanoribbons. ACS Applied Electronic Materials, 2020, 2, 1449-1458. | 4.3 | 1 |

| # | Article | IF | CITATIONS |
|----|--|-------------------------|---------------|
| 37 | Phographene as a High-Performance Anode Material with High Specific Capacity and Fast Li Diffusion: From Structural, Electronic, and Mechanical Properties to LIB Applications. Journal of Physical Chemistry C, 2019, 123, 21345-21352. | 3.1 | 43 |
| 38 | Unraveling the controversy over a catalytic reaction mechanism using a new theoretical methodology: One probe and non-equilibrium surface Green's function. Nano Energy, 2019, 63, 103863. | 16.0 | 7 |
| 39 | Enhanced catalytic activity of SO _x -incorporated graphene for the hydrogen evolution reaction. Journal of Materials Chemistry A, 2019, 7, 22615-22620. | 10.3 | 4 |
| 40 | Atomistic insights into the anisotropic mechanical properties and role of ripples on the thermal expansion of h-BCN monolayers. RSC Advances, 2019, 9, 1238-1246. | 3.6 | 38 |
| 41 | Unveiling dual-linkage 3D hexaiminobenzene metal–organic frameworks towards long-lasting advanced reversible Zn–air batteries. Energy and Environmental Science, 2019, 12, 727-738. | 30.8 | 300 |
| 42 | B ₃ S monolayer: prediction of a high-performance anode material for lithium-ion batteries. Journal of Materials Chemistry A, 2019, 7, 12706-12712. | 10.3 | 59 |
| 43 | Two-dimensional haeckelite h567: A promising high capacity and fast Li diffusion anode material for lithium-ion batteries. Carbon, 2019, 148, 344-353. | 10.3 | 59 |
| 44 | Time Transient Electrochemical Monitoring of Tetraalkylammonium Polybromide Solid Particle Formation: Observation of Ionic Liquid-to-Solid Transitions. Analytical Chemistry, 2019, 91, 5850-5857. | 6.5 | 13 |
| 45 | Metal-Free Oxygen Evolution and Oxygen Reduction Reaction Bifunctional Electrocatalyst in Alkaline Media: From Mechanisms to Structure–Catalytic Activity Relationship. ACS Sustainable Chemistry and Engineering, 2018, 6, 4973-4980. | 6.7 | 62 |
| 46 | Theoretical investigation on the ground state properties of the hexaamminecobalt(<scp>iii</scp>) and nitro–nitrito linkage isomerism in pentaamminecobalt(<scp>iii</scp>) <i>in vacuo</i> . RSC Advances, 2018, 8, 3328-3342. | 3.6 | 11 |
| 47 | Three-dimensional evaluation of compositional and structural changes in cycled LiNi1/3Co1/3Mn1/3O2 by atom probe tomography. Journal of Power Sources, 2018, 379, 160-166. | 7.8 | 23 |
| 48 | Hierarchically Designed 3D Holey C ₂ N Aerogels as Bifunctional Oxygen Electrodes for Flexible and Rechargeable Zn-Air Batteries. ACS Nano, 2018, 12, 596-608. | 14.6 | 159 |
| 49 | Adjustable Intermolecular Interactions Allowing 2D Transition Metal Dichalcogenides with Prolonged Scavenging Activity for Reactive Oxygen Species. Small, 2018, 14, e1800026. | 10.0 | 30 |
| 50 | Molecular layer deposition of charge-transfer complex thin films with visible-light absorption. Organic Electronics, 2018, 52, 237-242. | 2.6 | 4 |
| 51 | Atomistic Dynamics Investigation of the Thermomechanical Properties and Li Diffusion Kinetics in Ĩ^-Graphene for LIB Anode Material. ACS Applied Materials & Interfaces, 2018, 10, 36240-36248. | 8.0 | 39 |
| 52 | Rational design of time-resolved turn-on fluorescence sensors: exploiting delayed fluorescence for hydrogen peroxide sensing. Chemical Communications, 2018, 54, 12069-12072. | 4.1 | 25 |
| 53 | Radical Scavengin: Environmental Stimuliâ€rresponsive Longâ€Term Radical Scavenging of 2D Transition Metal Dichalcogenides through Defectâ€Mediated Hydrogen Atom Transfer in Aqueous Media (Adv.) Tj ETQq1 I | 1 0. ₮&9 314 | ⊦rgƁT /Overlo |
| 54 | Palladium atalyzed Carbonylative Coupling Reactions of <i>N</i> , <i>N</i> â€Bis(methanesulfonyl)amides through C–N Bond Cleavage. European Journal of Organic Chemistry, 2018, 2018, 5717-5724. | 2.4 | 13 |

| # | Article | IF | CITATIONS |
|----|---|------|-----------|
| 55 | Environmental Stimuliâ€Irresponsive Longâ€Term Radical Scavenging of 2D Transition Metal Dichalcogenides through Defectâ€Mediated Hydrogen Atom Transfer in Aqueous Media. Advanced Functional Materials, 2018, 28, 1802737. | 14.9 | 9 |
| 56 | 2D transition metal dichalcogenides with glucan multivalency for antibody-free pathogen recognition. Nature Communications, 2018, 9, 2549. | 12.8 | 44 |
| 57 | Solidâ€&tate Rechargeable Zinc–Air Battery with Long Shelf Life Based on Nanoengineered Polymer Electrolyte. ChemSusChem, 2018, 11, 3215-3224. | 6.8 | 55 |
| 58 | Assessment of the mechanical properties of monolayer graphene using the energy and strain-fluctuation methods. RSC Advances, 2018, 8, 27283-27292. | 3.6 | 42 |
| 59 | <i>Nido</i> â€Carboranes: Donors for Thermally Activated Delayed Fluorescence. Angewandte Chemie - International Edition, 2018, 57, 12483-12488. | 13.8 | 70 |
| 60 | <i>Nido</i> arboranes: Donors for Thermally Activated Delayed Fluorescence. Angewandte Chemie, 2018, 130, 12663-12668. | 2.0 | 24 |
| 61 | Efficiency Tuning of UVA/UVB Absorbance through Control over the Intramolecular Hydrogen Bonding of Triazine Derivatives. Bulletin of the Korean Chemical Society, 2018, 39, 858-863. | 1.9 | 1 |
| 62 | p- and n-type Doping Effects on the Electrical and Ionic Conductivities of Li4Ti5O12 Anode Materials. Journal of Physical Chemistry C, 2018, 122, 15155-15162. | 3.1 | 10 |
| 63 | Quantitative Correlation between Carrier Mobility and Intermolecular Center-to-Center Distance in Organic Single Crystals. Chemistry of Materials, 2017, 29, 4072-4079. | 6.7 | 12 |
| 64 | Scalable 3-D Carbon Nitride Sponge as an Efficient Metal-Free Bifunctional Oxygen Electrocatalyst for Rechargeable Zn–Air Batteries. ACS Nano, 2017, 11, 347-357. | 14.6 | 369 |
| 65 | Theoretical evaluation of the structure–activity relationship in graphene-based electrocatalysts for hydrogen evolution reactions. RSC Advances, 2017, 7, 27033-27039. | 3.6 | 21 |
| 66 | Deciphering the Electrocatalytic Activity of Nitrogen-Doped Carbon Embedded with Cobalt Nanoparticles and the Reaction Mechanism of Triiodide Reduction in Dye-Sensitized Solar Cells. Journal of Physical Chemistry C, 2017, 121, 27332-27343. | 3.1 | 18 |
| 67 | Controlled Growth of Rubrene Nanowires by Eutectic Melt Crystallization. Scientific Reports, 2016, 6, 23108. | 3.3 | 11 |
| 68 | Exploring Interfacial Events in Gold-Nanocluster-Sensitized Solar Cells: Insights into the Effects of the Cluster Size and Electrolyte on Solar Cell Performance. Journal of the American Chemical Society, 2016, 138, 390-401. | 13.7 | 137 |
| 69 | Aromatic cages B0/+42: unprecedented existence of octagonal holes in boron clusters. Physical Chemistry Chemical Physics, 2016, 18, 11620-11623. | 2.8 | 16 |
| 70 | Behavior of maltose-neopentyl glycol-3 (MNG-3) at the air/aqueous interface. Colloids and Surfaces A: Physicochemical and Engineering Aspects, 2015, 484, 184-189. | 4.7 | 0 |
| 71 | Two Dimensional Aggregation Behaviors of Quinoxaline Dendrimers. Journal of Nanoscience and Nanotechnology, 2015, 15, 1511-1514. | 0.9 | 1 |
| 72 | Manipulation of Phosphorescence Efficiency of Cyclometalated Iridium Complexes by Substituted <i>o</i> â€Carboranes. Chemistry - A European Journal, 2015, 21, 2052-2061. | 3.3 | 70 |

| # | Article | IF | CITATIONS |
|----|---|------|-----------|
| 73 | <i>o</i> -Carboranyl–Phosphine as a New Class of Strong-Field Ancillary Ligand in Cyclometalated Iridium(III) Complexes: Toward Blue Phosphorescence. Organometallics, 2015, 34, 3455-3458. | 2.3 | 38 |
| 74 | Iridium Cyclometalates with Tethered <i>o</i> -Carboranes: Impact of Restricted Rotation of <i>o</i> -Carborane on Phosphorescence Efficiency. Journal of the American Chemical Society, 2015, 137, 8018-8021. | 13.7 | 103 |
| 75 | Selective Synthesis of Ruthenium(II) Metalla[2]Catenane via Solvent and Guest-Dependent Self-Assembly. Journal of the American Chemical Society, 2015, 137, 4674-4677. | 13.7 | 97 |
| 76 | Strain Energy and Structural Property of Methyl Substituted Imogolite. Molecular Crystals and Liquid Crystals, 2014, 599, 68-71. | 0.9 | 3 |
| 77 | Doubling the Capacity of Lithium Manganese Oxide Spinel by a Flexible Skinny Graphitic Layer. Angewandte Chemie - International Edition, 2014, 53, 5059-5063. | 13.8 | 25 |
| 78 | Terpyridine–Triarylborane Conjugates for the Dual Complexation of Zinc(II) Cation and Fluoride Anion. Organometallics, 2014, 33, 753-762. | 2.3 | 35 |
| 79 | Synthesis and characterization of an ester-terminated organic semiconductor for ethanol vapor detection. Organic Electronics, 2014, 15, 2277-2284. | 2.6 | 6 |
| 80 | Thermodynamic Control of Diameter-Modulated Aluminosilicate Nanotubes. Journal of Physical Chemistry C, 2014, 118, 8148-8152. | 3.1 | 16 |
| 81 | Experimental and theoretical investigation of fluorine substituted LiFe0.4Mn0.6PO4 as cathode material for lithium rechargeable batteries. Solid State Ionics, 2014, 260, 2-7. | 2.7 | 27 |
| 82 | Synthesis and Characteristics of a Biobased High- <i>T</i> _g Terpolyester of Isosorbide, Ethylene Glycol, and 1,4-Cyclohexane Dimethanol: Effect of Ethylene Glycol as a Chain Linker on Polymerization. Macromolecules, 2013, 46, 7219-7231. | 4.8 | 113 |
| 83 | Preparation of an imogolite/poly(acrylic acid) hybrid gel. Journal of Colloid and Interface Science, 2013, 406, 165-171. | 9.4 | 21 |
| 84 | Opening and blocking the inner-pores of halloysite. Chemical Communications, 2013, 49, 4519. | 4.1 | 74 |
| 85 | ENANTIOMER SEPARATION OF <i>N</i> -t-BOC AND <i>N</i> -CBZ α-AMINO ACIDS AND THEIR ESTERS ON POLYSACCHARIDE DERIVED CHIRAL STATIONARY PHASES. Journal of Liquid Chromatography and Related Technologies, 2013, 36, 1899-1914. | 1.0 | 1 |
| 86 | Temperature Effect on the Synthesis of Gibbsite and Boehmite. Chemistry Letters, 2013, 42, 1463-1465. | 1.3 | 3 |
| 87 | Influence of Exchange-Correlation Functional in the Calculations of Vertical Excitation Energies of Halogenated Copper Phthalocyanines using Time-Dependent Density Functional Theory (TD-DFT). Bulletin of the Korean Chemical Society, 2013, 34, 2276-2280. | 1.9 | 9 |
| 88 | Chiral Recognition of <i>N</i> â€Phthaloyl, <i>N</i> â€Tetrachlorophthaloyl, and <i>N</i> â€Naphthaloyl αâ€Amino Acids and Their Esters on Polysaccharideâ€Derived Chiral Stationary Phases. Chirality, 2012, 24, 1037-1046. | 2.6 | 19 |
| 89 | Aggregation and Stabilization of Carboxylic Acid Functionalized Halloysite Nanotubes (HNT-COOH). Journal of Physical Chemistry C, 2012, 116, 18230-18235. | 3.1 | 97 |
| 90 | Origin of the Strain Energy Minimum in Imogolite Nanotubes. Journal of Physical Chemistry C, 2011, 115, 5226-5231. | 3.1 | 30 |

| # | Article | IF | CITATIONS |
|-----|---|------|-----------|
| 91 | Metal Ion Coordination with an Asymmetric Fan-Shaped Dendrimer at the Air–Water Interface. Langmuir, 2011, 27, 8898-8904. | 3.5 | 8 |
| 92 | Electron transport characteristics of organic molecule encapsulated carbon nanotubes. Nanoscale, 2011, 3, 1773. | 5.6 | 10 |
| 93 | The Origin of the Halogen Effect on the Phthalocyanine Green Pigments. Chemistry - an Asian Journal, 2010, 5, 1341-1346. | 3.3 | 4 |
| 94 | Carbon Nanotubes Oscillation under Electric Field. Japanese Journal of Applied Physics, 2010, 49, 115103. | 1.5 | 2 |
| 95 | Electron transport characteristics of one-dimensional heterojunctions with multi-nitrogen-doped capped carbon nanotubes. Nanoscale, 2010, 2, 2758. | 5.6 | 8 |
| 96 | Rigid adamantane tripod linkage for well-defined conductance of a single-molecule junction. Physical Chemistry Chemical Physics, 2010, 12, 11763. | 2.8 | 12 |
| 97 | Designing Nanogadgetry for Nanoelectronic Devices with Nitrogenâ€Doped Capped Carbon Nanotubes. Small, 2009, 5, 1769-1775. | 10.0 | 176 |
| 98 | The Role of Aromaticity and the <i>Ï€</i> â€Conjugated Framework in Multiporphyrinic Systems as Singleâ€Molecule Switches. Small, 2008, 4, 962-969. | 10.0 | 26 |
| 99 | Electron transport through carbon nanotube intramolecular heterojunctions with peptide linkages. Physical Chemistry Chemical Physics, 2008, 10, 5225. | 2.8 | 16 |
| 100 | Designing Nanogadgets by Interconnecting Carbon Nanotubes with Zinc Layers. ACS Nano, 2008, 2, 939-943. | 14.6 | 20 |
| 101 | Structural Dependence of Magnetic Shielding Properties in Al ₄ Li ₄ Clusters. Materials Transactions, 2008, 49, 2429-2436. | 1.2 | 1 |
| 102 | Transport Properties of Nanoscale Materials for Molecular Wire Applications: A Case Study of Ferrocene Dimers. Journal of the Korean Physical Society, 2008, 52, 1197-1201. | 0.7 | 10 |
| 103 | Computational Design of a Rectifying Diode Made by Interconnecting Carbon Nanotubes with Peptide Linkages. Journal of Physical Chemistry C, 2007, 111, 12175-12180. | 3.1 | 24 |
| 104 | Control of Electron Transport by Manipulating the Conjugated Framework. Journal of Physical Chemistry C, 2007, 111, 15397-15403. | 3.1 | 22 |
| 105 | Interpreting STM image and tunneling-current-induced rotation of cis-2-butene on a Pd(110) surface. Chemical Physics Letters, 2007, 435, 90-95. | 2.6 | 3 |
| 106 | Thermal cis–trans isomerization of triazo-benzene. Current Applied Physics, 2007, 7, 513-516. | 2.4 | 2 |
| 107 | Molecular dynamics study of the ionic conductivity of 1-n-butyl-3-methylimidazolium salts as ionic liquids. Chemical Physics Letters, 2005, 406, 332-340. | 2.6 | 88 |
| 108 | Density Functional Studies of Ring-Opening Reactions of Li ⁺ -(ethylene carbonate) and Li ⁺ -(vinylene carbonate). Bulletin of the Korean Chemical Society, 2005, 26, 43-46. | 1.9 | 7 |

5

| # | Article | IF | CITATIONS |
|-----|--|-----|-----------|
| 109 | Structure and stability of the defect fullerene clusters of C60: C59, C58, and C57. Journal of Chemical Physics, 2004, 121, 3941-3942. | 3.0 | 31 |
| 110 | Performance of density functionals for calculation of reductive ring-opening reaction energies of Li + -EC and Li + -VC. Theoretical Chemistry Accounts, 2004, 112, 106-112. | 1.4 | 31 |
| 111 | Density functional calculations on the ionization potentials of (CuPc)n (n=1–6). Computational and Theoretical Chemistry, 2004, 672, 231-234. | 1.5 | 8 |
| 112 | Two-dimensional packing patterns of amino acid surfactant and higher alcohols in an aqueous phase and their associated packing parameters. Journal of Colloid and Interface Science, 2004, 273, 596-603. | 9.4 | 11 |
| 113 | Time-dependent density-functional calculations of S[sub 0]–S[sub 1] transition energies of poly(p-phenylene vinylene). Journal of Chemical Physics, 2004, 121, 609. | 3.0 | 19 |
| 114 | New catalyst design for polymerization of norbornene esters by reducing intramolecular interaction. Journal of Molecular Modeling, 2003, 9, 304-307. | 1.8 | 4 |
| 115 | Enantiomeric discrimination of pyrethroic acid esters on polysaccharide derived chiral stationary phases. Chirality, 2003, 15, 276-283. | 2.6 | 15 |
| 116 | Theoretical studies of the solvent decomposition by lithium atoms in lithium-ion battery electrolyte. Chemical Physics Letters, 2002, 360, 359-366. | 2.6 | 44 |
| 117 | Molecular orbital study on the ground and excited states of methyl substituted tris(8-hydroxyquinoline) aluminum(III). Chemical Physics Letters, 2002, 366, 9-16. | 2.6 | 44 |
| | | | |

118 Theoretical Basis of Electrocatalysis. , 0, , .